Journal of Non-Crystalline Solids 513 (2019) 137–143

Contents lists available at ScienceDirect

Journal of Non-Crystalline Solids

journal homepage: www.elsevier.com/locate/jnoncrysol

Very low density amorphous phase of zircon

Süleyman Bolat[a], Murat Durandurdu[b,*]

[a] Faculty of Science, Department of Physics, Karadeniz Technical University, Trabzon 61080, Turkey
[b] Department of Materials Science & Nanotechnology Engineering, Abdullah Gül University, Kayseri 38080, Turkey

ARTICLE INFO

Keywords:
Amorphous
Zircon
Polymerization

ABSTRACT

Using a reliable *ab initio* molecular dynamics method, we investigate the rapid solidification of the zircon melt. Accompanied by amorphization, a drastic volume expansion of 27% is perceived. This value is fairly larger than 18% observed in the metamict zircon. Such a large volume swelling leads to a significant decrease in the mean coordination number of Zr atoms, which is about 5.66 and the lowest one reported so far. On the other hand, the volume expansion is found to have almost no impact on the average coordination number of Si atoms *i.e.*, they maintain their tetragonal coordination. As suggested by earlier investigations, the polymerization of SiO_4 units is witnessed but our model shows the highest polymerization with respect to the previous simulations. Based on our findings, we propose that our model does not represent the metamict zircon but a very low density amorphous phase of zircon.

1. Introduction

Zircon ($ZrSiO_4$) is an important mineral and used as gemstone for about 2000 years. Especially colorless zircon is sometimes used as alternative for diamond [1]. Zircon has a high hardness, a high melting temperature, high thermal conductivity and good chemical stability, which make it an attractive source of materials science. Additionally, it can be used in the nuclear platform and even in the laser industry [2–5].

Zircon has an orthosilicate structure with a tetragonal symmetry. This mineral has an $I4_1/amd$ space group with the lattice parameters $a = b = 6.607$ Å and $c = 5.981$ Å, in which Zr^{4+} and Si^{4+} are on the position of cations with $\bar{4}2m$ symmetry. Each Zr atom constitutes the ZrO_8 polyhedron having the [Zr−O] bond lengths of 2.13/2.27 Å. In the polyhedron, the [O−O] distances are 2.43 Å along the edge shared and 2.75 Å along the unshared edge, and the angles between the O atoms and the Zr atom are 64.8°, 69.0°, 80.4° and 92.2°. Each Si atom has 4 O neighbors at 1.62 Å, and the angles between O atoms and Si atom are 97° and 116° [6–9]. The high pressure phase of zircon with the scheelite structure was first synthesized in laboratory conditions by Reid and Ringwood [10]. The scheelite-crystal has the space group of $I4_1/a$ with the lattice parameters of $a = b = 4.738$ Å and $c = 10.51$ Å. Accompanied by the phase change, the density increases about 10% [10,11]. The critical pressure for this phase transformation was reported to be around 12 GPa at a temperature of 1073 K. For natural zircon, in shock wave experiments at room temperature, the phase transformation was observed at a pressure of about 30 GPa [12] while for synthetic pure zircon, the onset of the phase transition was perceived at a pressure of 20 GPa [13]. The transition pressure is sufficiently affected by temperature, as expected, because temperature generally accelerates phase transitions [10]. The scheelite structured zircon was found to be highly incompressible. Therefore it can serve as an ultrahard material [14]. More information about zircon and zircon type oxides and their high pressure behavior can be found in a recent review paper [15].

Natural amorphous zircon, a product of the accumulation of radiation damage over years, is also of interest. It mainly consists of amorphous and crystalline domains and is commonly referred as the metamict state. The local structure of the crystalline and amorphous domains in the metamict zircon appears to depend on the radiation dose and radiation time [16]. Due to the amorphization, the physical and mechanical properties of zircon change severely [16] such that the amorphization leads to a considerably volume expansion (18%) [17], the polymerization of SiO_4 units and a decrease in Zr coordination from 8 to about 7 [18].

Amorphous zircon can be experimentally prepared by using heavy ions, reactive magnetron sputtering and sol-gel processing as well [19–21]. The melt and quench technique seems to be not successful in producing amorphous zircon because it leads to the formation of zirconia crystal and amorphous silica [22]. It should be pointed out here that natural and experimentally produced amorphous zircons show remarkable resemblances.

In order to have information about amorphous zircon at the

* Corresponding author.
E-mail address: murat.durandurdu@agu.edu.tr (M. Durandurdu).

https://doi.org/10.1016/j.jnoncrysol.2019.03.023
Received 26 December 2018; Received in revised form 14 March 2019; Accepted 14 March 2019
Available online 28 March 2019
0022-3093/

atomistic level, classical [23,24] and *ab initio* [25] molecular dynamics (MD) simulations were carried out. In both approaches, the amorphous models were generated using the melt and quenching technique. In the classical MD simulation [23], when a NPT ensemble was used, about 11% volume expansion was observed after cooling the zircon melt to 300 K, which is quite less than 18% swelling observed in the metamict zircon. In the same classical MD study, a NVT ensemble with an 18% volume enlargement was also performed. In the *ab initio* MD simulation, similarly amorphous zircon with two different densities was created. Although there are some distinctions about the data provided in these simulations, they have delivered valuable knowledge about the short-range of amorphous zircon.

Here we model amorphous zircon using an *ab initio* MD technique that was successful in generating amorphous zirconia. Relative to the previous *ab initio* MD calculations, we use a larger simulation cell, a longer simulation time and a NPT ensemble in the present study. We find that the volume expansion is 27% for our amorphous model and the mean coordination number of Zr atoms is around 5.66. On the basis of our observations, we propose that there might exist a very low density amorphous form of zircon.

2. Methodology

The *ab initio* MD simulations were performed by the SIESTA code [26]. For the simulations, double-zeta plus (DZP) polarization orbitals were chosen. Temperature and pressure were controlled by the velocity rescaling method and the Parrinello-Rahman method, respectively [27]. For the exchange-correlation energy, the generalized gradient approximation (GGA) of Perdew, Burke and Ernzerhof was opted [28]. The Trouller-Martins scheme was used to create pseudopotentials [29]. The zircon crystal (tetragonal symmetry $I4_1/amd$) consisting of 192 atoms (32 Zr atoms, 32 Si atoms and 128 O atoms) as shown in Fig. 1 were chosen as an initial structure with the periodic boundary conditions and relaxed using a conjugate gradient technique. The lattice parameters and the atomic positions of the relaxed structure obtained using the KPLOT program [30] are provided in Table 1. As can be seen from the table, our results are comparable with experiments [9]. Each MD step was set to be one fs. After the relaxation, the crystal was subjected to a high temperature of 4000 K for 18 ps. Then it was cooled down to 2600 K in 3 ps and equilibrated for approximately 18 ps at this temperature. Noted that the melting temperature of zircon is about 2475–2825 K [31]. Yet it was reported that at temperatures in the range 1775–2275 K, zircon could undergo separation into zirconia and SiO_2 [32], suggesting the occurrence of high diffusivity in zircon at temperatures even below its melting point. In order to see whether the structure at 2600 K exhibited the dynamics of a liquid state, we performed a constant volume simulation, run additional 1000 MD steps and computed the mean square displacement (MSD) using the ISAACS program [33]. The estimated MSD is provided in Fig. 2. From the linear fitting between 150 and 400 fs, the diffusion constant D (using the Einstein relation, $\langle (r(t) - r(0))^2 \rangle = 6tD$) was estimated to be $\sim 9 \times 10^{-5}$ cm^2 /s. In the final step, the temperature applied was reduced gradually to 300 K in 63 ps. The variation of temperature and pressure as a function of MD time during the whole simulation processes is illustrated in Fig. 3.

Table 1
The lattice parameters and the atomic positions of the relaxed zircon crystal.

	Lattice Parameters					
	present work			[9] (experimental ref.)		
	a (Å)	*b* (Å)	*c* (Å)	*a* (Å)	*b* (Å)	*c* (Å)
	6.660	6.660	6.067	6.604	6.604	5.980
	Fractional Position					
	present work			[9] (experimental ref.)		
	x	*y*	*z*	*x*	*y*	*z*
Zr (4*a*)	0.0000	0.7500	0.1250	0.0000	0.7500	0.1250
Si (4*b*)	0.0000	0.7500	0.6250	0.0000	0.7500	0.6250
O (16*h*)	0.0000	0.0647	0.1940	0.0000	0.0660	0.1951

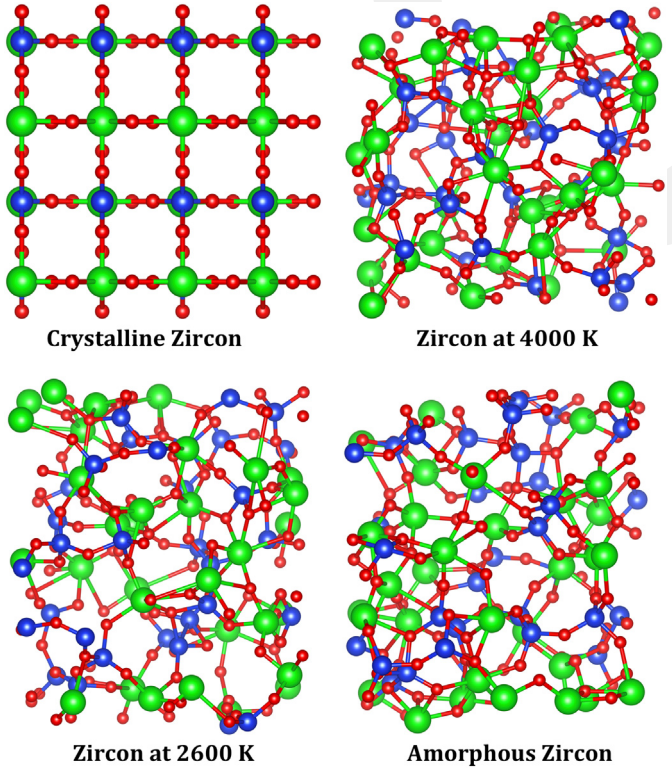

Fig. 1. The ball stick representation of the crystalline and disordered zircon structures having 192 atoms.

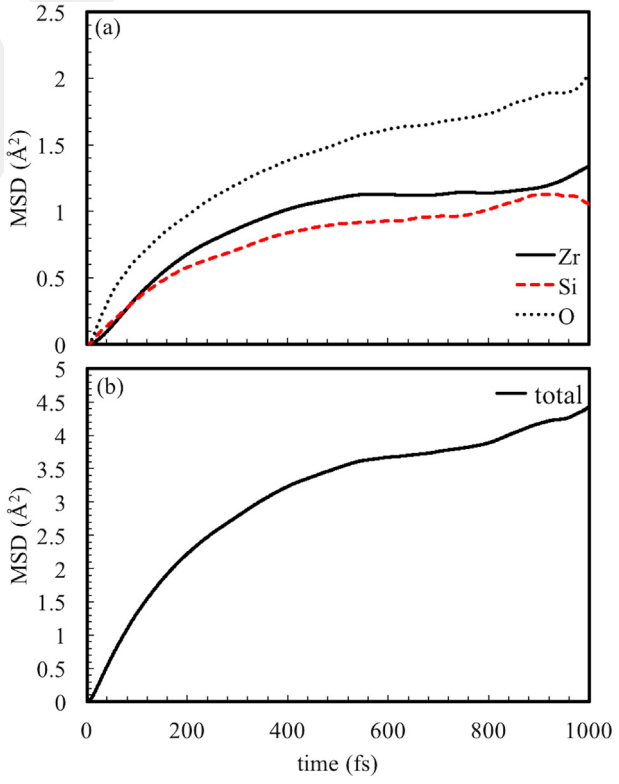

Fig. 2. Mean square displacement at 2600 K.

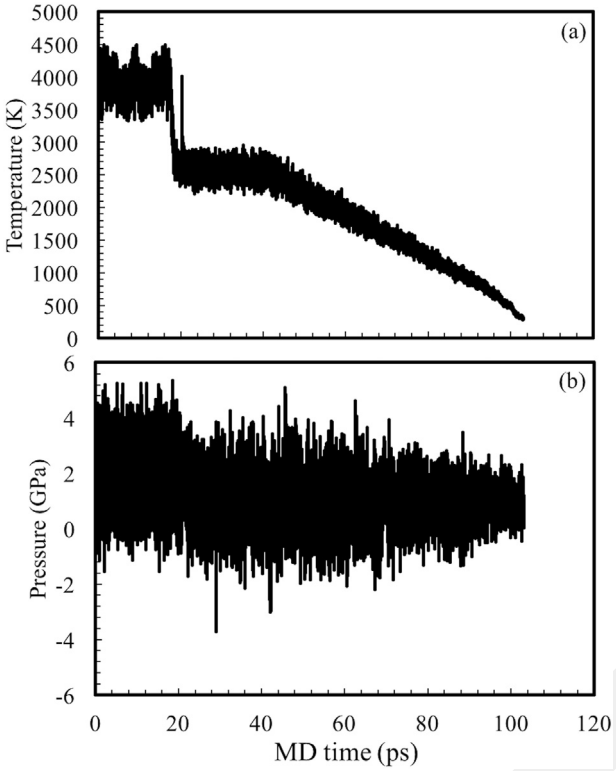

Fig. 3. Variation of temperature and pressure as a function of MD time.

3. Results

Fig. 4 shows the volume per atom of the zircon system *versus* the temperature applied. As can be evidently seen from the figure, the volume decreases during the quenching process and a critical glass transition zone is observed, suggesting a glass-transition temperature (T_g) between 1650 K and 1750 K for zircon. This value is, however, fairly less than the value of 2000 K proposed in the classical MD simulation [23].

The cation-anion pair distribution functions (PDFs) of the amorphous and crystalline structures of zircon are illustrated in Fig. 5. One can see that the position of the first peak of almost all correlations of the non-crystalline state is different than that in the crystal. The [Zr—O] bond length in the crystal is located at 2.15/ 2.29 Å, which is comparable with the experimental and theoretical results of 2.13/2.27 Å as seen in Table 1. Similar to the earlier investigations, the [Zr—O] distance somewhat decreases by amorphization. In the present work, it is estimated to be 2.0 Å, which is less than the values of 2.07–2.13 Å

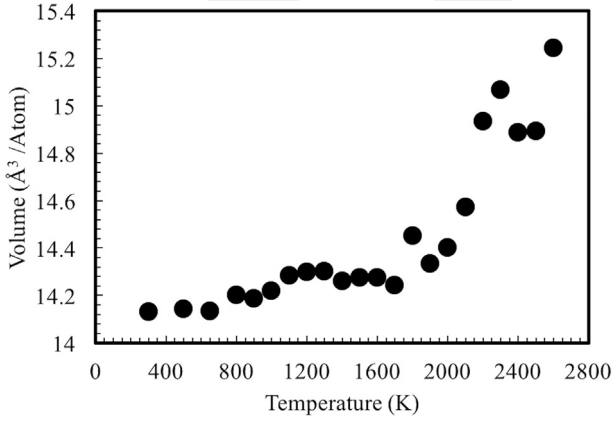

Fig. 4. The volume per atom *versus* temperature of zircon system.

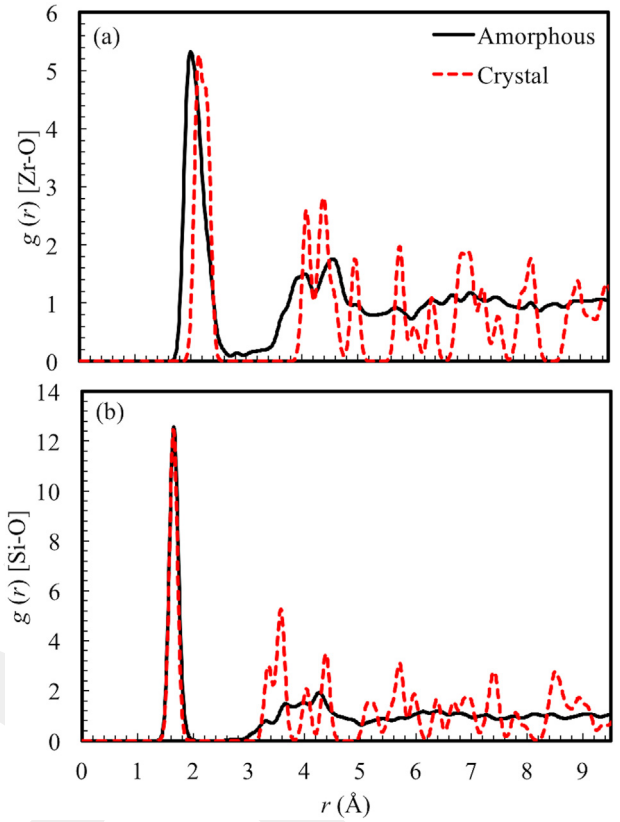

Fig. 5. The cation-anion pair distribution functions (PDFs) of the amorphous and crystalline zircon. The peak intensity of the crystal structure was scaled to the peak intensity value of amorphous structure for clarity.

reported for the amorphous/metamict zircon [25]. The [Si—O] bond separation, on the other hand, increases from 1.64 to 1.65 Å by amorphization. Such an increase was reported in the previous *ab initio* simulation from 1.62 Å (crystal) to 1.68 Å (amorphous) [25] but not in the classical MD simulation in which the Si—O distance decreased from 1.62 (crystal) to 1.59–1.60 Å (high and low density amorphous states, respectively) [23]. Our [Si—O] bond length is indeed in good agreement with the experimental result of 1.64 Å [34].

The cation-cation PDFs are shown in Fig. 6. We witness the splitting in the [Zr—Zr] separation. The first and second peaks are positioned at ~3.48 and 3.95 Å, respectively, which are shorter and longer than the 3.65 Å of the [Zr—Zr] first peak in the crystal. Such a splitting was also experienced in the classical MD simulation [23,24] and it was attributed to the presence of edge and corner sharing ZrO_x polyhedra, which contribute to the second and first peaks of [Zr-Zr] correlation, correspondingly. Furthermore, the shortening of the correlation can be attributed to a decrease in the [Zr—O] coordination number as well. Note that the crystal consists of only edge sharing polyhedrons. We need to point out here that the main difference between the present study and the empirical simulation is the intensity of the first peak: it is less than the second one in our simulation while the opposite trend can be seen in the empirical simulation [23], suggesting that our model consists of more edge sharing ZrO_x polyhedrons than the empirical model. The [Si—Si] correlation also decreases from 3.65 Å in the crystal to 3.09 Å in the amorphous state, in agreement with the earlier investigations (see Table 2). Such a decrease can be attributed to the polymerization of [Si—O] configurations. The first two peaks of [Zr—Si] correlation in the crystal are located at 3.01 Å and 3.47 Å and are due to the edge sharing and corner sharing SiO_4 and ZrO_8 units, respectively. In the amorphous model, these two peaks overlap and produce a broad peak with a shoulder. The peak and shoulder are located at 3.03 Å and 3.65 Å, correspondingly. Such an observation also agrees with the previous MD

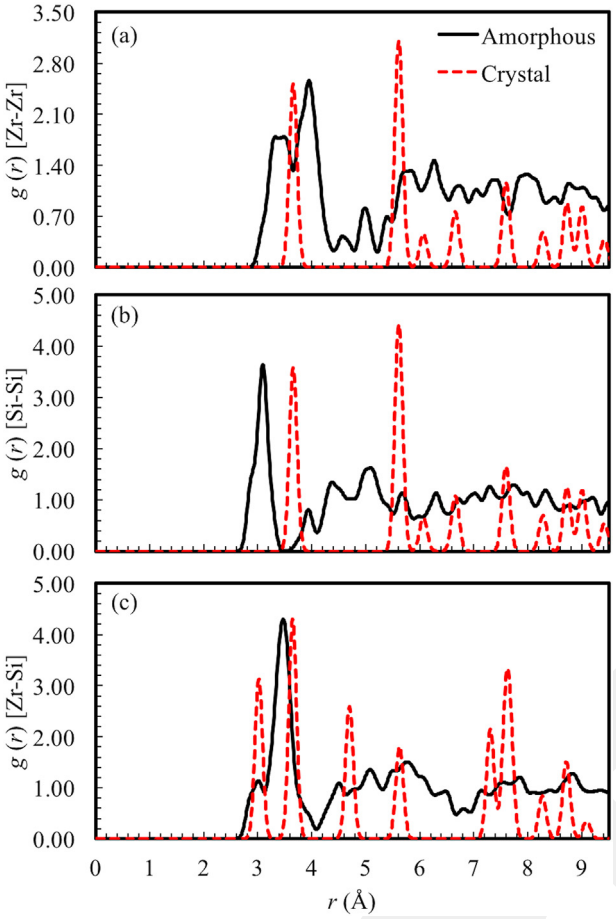

Fig. 6. The cation-cation PDFs of the amorphous and crystalline zircon. The peak intensity of the crystal structure was scaled to the peak intensity value of amorphous structure for clarity.

Table 2
Comparison the correlation distances (Å).

Structure	Ref.	Zr–O	Si–O	Zr–Zr	Si–Si	Zr–Si
Amorphous	present work	2.00	1.65	3.48/3.95	3.09	3.01/3.47
Amorphous	[34][a]	2.13/2.24	1.64	–	–	–
Amorphous	[25][b]	2.07	1.68		3.10	
Amorphous	[23][c]	2.10	1.60	3.42/3.85	3.13	3.48
Crystal	present work	2.15/2.27	1.64	3.65	3.65	3.03/3.65
Crystal	[25][b]	2.13/2.27	1.62			
Crystal	[9][a]	2.13/2.27	1.62	–	–	–
Crystal	[6][a]	2.13/2.27	–	3.63	–	2.99/3.63
Crystal	[34][a]	2.12/2.25	1.61	–	–	–
Crystal	[37][a]	2.13/2.27	–	3.66	–	2.99/3.66
Crystal	[3][a]	2.13	1.62	–	–	–
Crystal	[23][c]	2.13/2.27	1.62	3.61	3.61	2.99/3.63
Crystal	[24][d]	2.13/2.30	1.64	–	–	–
Crystal	[35][e]	2.11	1.61	–	–	–
Crystal	[36][f]	2.16/2.36	1.59	–	–	–
Crystal	[36][g]	2.11/2.26	1.62	–	–	–

[a] Experimental.
[b] *ab initio* MD simulation.
[c] Classical MD simulation.
[d] Classical MD simulation (DLPOLY code).
[e] Quantum mechanical calculation.
[f] BMH empirical potential.
[g] DFT-LDA *ab initio*.

simulation and XRD results [34,38].

Depending on temperature, we use the cutoff radii of ~2.10–2.39 Å for the [Si–O] correlation and ~2.91–3.17 Å for the [Zr–O] pairs to determine the average total/partial coordination numbers (CNs). The variation of mean CNs of the system as a function of temperature is given in Fig. 7. From the figure, it can be understood that the CNs are not very sensitive to temperature. The mean CN of Zr, Si and O atoms in the amorphous (liquid) structure is 5.66 (5.84), 4.06 (3.94) and 2.43 (2.45) respectively. Consequently, in the amorphous phase we find a drastic decrease in the mean CN of Zr and O atoms while Si atoms retain almost the same mean CN in both amorphous and crystalline phases. Indeed, a decrease in the mean CN of Zr atoms was also stated in the earlier experimental and theoretical studies [23,39]. However our value is noticeably less than the simulation results of 6–7 [23] and 7.2 [39] found for amorphous zircon and experimental result of about 7 determined for the metamict zircon [18]. The coordination distribution of each species is given in Fig. 8. In the amorphous state, the five-fold and six-fold coordinated Zr atoms are dominant with a frequency of 41% and 44%, respectively. The fraction of four-fold and seven-fold coordinated configurations are 3% and 12%, correspondingly. So one can see that the local structure of Zr atoms in the non-crystalline state is significantly different than that of Zr atoms in the crystal.

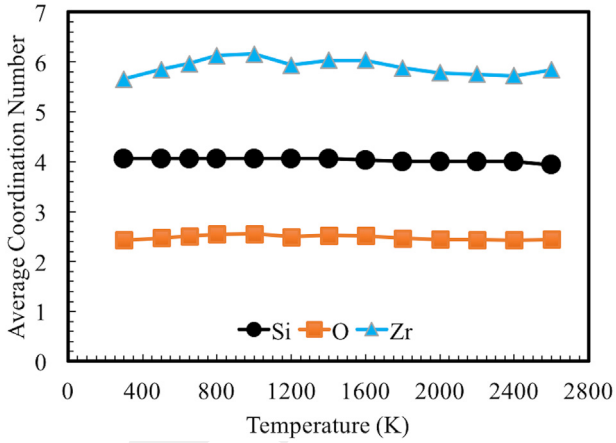

Fig. 7. The variation of average CNs of the zircon system as a function of temperature.

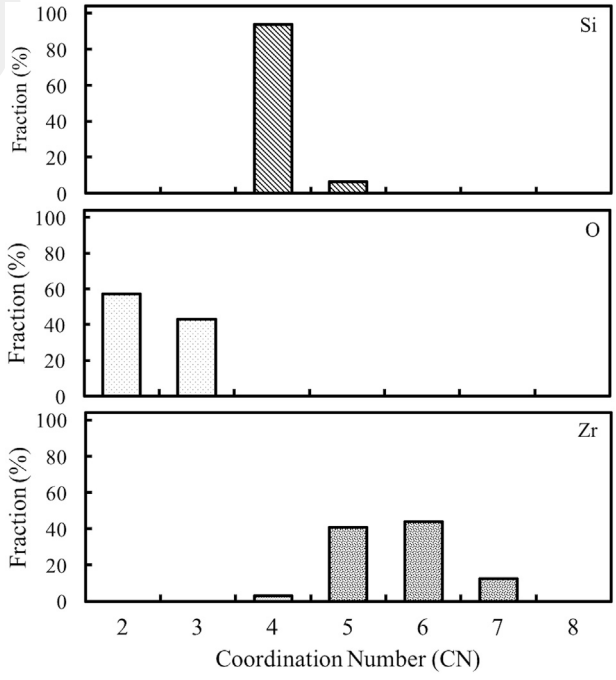

Fig. 8. The coordination distribution of each species.

Table 3
The Q_m^n units distribution in % for amorphous zircon.

	Q_4^0	Q_4^1	Q_4^2	Q_4^3	Q_4^4	Q_5^1
Present work	6.25	6.25	37.50	25.00	18.75	6.25
[23][a]	15.00	28.90	34.20	19.20	2.70	0
[23][b]	10.60	31.80	30.80	23.40	4.30	0
[24][c]	0	38.60	10.50	0	0	0
[24][d]	0	37.70	25.50	11.00	2.30	0

[a] Classical MD simulation of LD amorphous zircon.
[b] Classical MD simulation of HD amorphous zircon.
[c] Classical MD simulation (DLPOLY code) at 2200 K.
[d] Classical MD simulation (DLPOLY code) at 5000 K.

The earlier studies have revealed that amorphous zircon consists of numerous SiO_x units with either bridging oxygen atoms (BO) or non-bridging oxygen atoms (NBO). These building arrangements are characterized by Q_m^n units. Here m is the total number of BO and NBO atoms and n is the number of BO atoms. We find that n ranges from 0 to 4 and $n = 2$ is the most dominant cluster (37.5%) in our amorphous model (Table 3). Relative to the previous investigations, we have the lowest Q_4^0 and the highest Q_4^4 values. The mean Q_m^n value is 2.3 that is relatively higher than the values of 1.5–1.95 reported in the literature [23,24]. The higher n implies the greater SiO_4 polymerization. So our model shows more polymerized SiO_4 units than the other models.

Bond angle distribution functions (BADFs) of [O-Si-O], [O-Zr-O], [Si-O-Si] and [Zr-O-Zr] for the amorphous and crystalline structures are illustrated in Fig. 9 to compare their short-range order. The most apparent distinction is the occurrence of the [Si-O-Si] angles in the amorphous configuration in contrast to the crystal, which provides additional support to the polymerization of SiO_4 tetrahedra. The [Si-O-Si] angles range from 112° to 168° with sharp peaks positioned at about 120°, 141° and 162°. In a contrast to well separated peaks in the present work, the classical MD simulation produces a broad distribution with a peak at 145° and a minor peak at 155° [25]. In the glassy SiO_2, the [Si-O-Si] angles show a wide distribution from about 105° to 180° [40]. For the amorphous structure, the [O-Si-O] distribution exhibits a main peak at 109.3°, close to the ideal tetrahedral angle of 109.5° [40], indicating that the SiO_4 tetrahedra tends to be more symmetric. In the classical MD simulation [23] the main peak of [O-Si-O] distribution is located at 108°, in agreement with our result. The [Zr-O-Zr] angles have a very broad distribution having main peaks at around 100° and 126° for amorphous zircon while they produce sole peak at 111.4° for the crystal. Similarly, the [O-Zr-O] angles of the noncrystalline zircon create a wide distribution.

We finally compare the electronic structure of amorphous zircon with that of the crystalline zircon. Fig. 10 shows the calculated total and partial electron density of states of both zircon phases. The calculated HOMO-LUMO band gap energy of the crystal is 4.65 eV, which is comparable with the previous DFT calculation result of 4.87 eV [25] but quite less than the experimental data of 6.5 eV [41] because of the limitation of the DFT-GGA calculations. For the case of the amorphous form, the band gap energy is estimated to be 3.9 eV. Consequently, amorphization leads to a noticeable closure of band gap energy. The partial electron density of states reveal that the valance band states are mainly due to the O-atoms while the conduction band states are largely due to the Zr-atoms.

4. Discussion

All analyses disclose the fact that the amorphous and crystalline zircon phases have entirely different local structural arrangements. Although we find some overlaps between our results and the previous experimental and theoretical investigations, our mean CN of Zr atoms is the lowest one reported so far. The controversy between our calculation and experiments can be explained in terms of structural and density

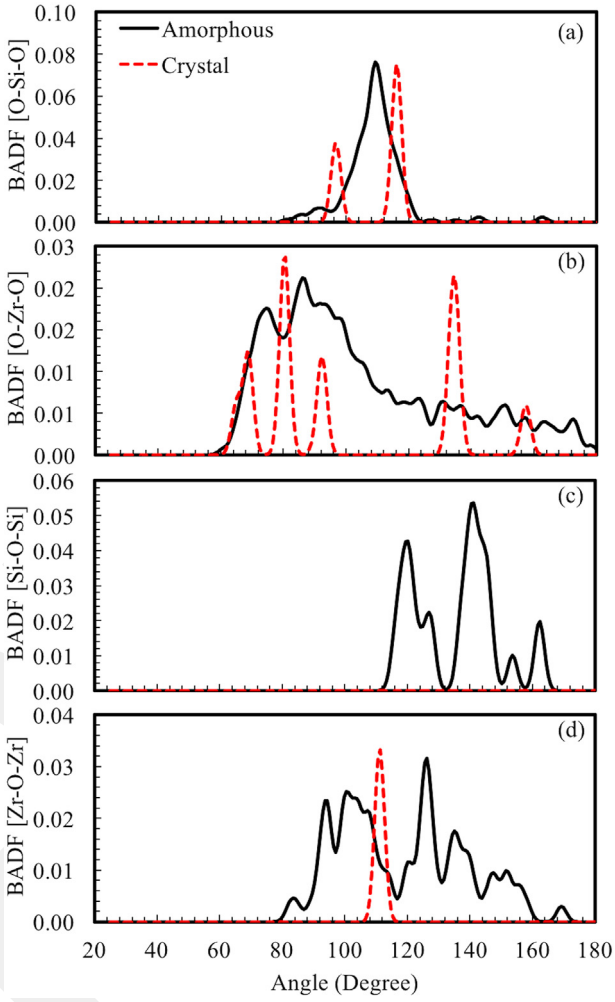

Fig. 9. Bond angle distribution functions (BADFs) for the amorphous and crystal structures of zircon. The peak intensity of the crystal structure for clarity was scaled to the peak intensity value of amorphous structure.

differences. Namely our model is completely amorphous while the experimental samples (metamict zircon) consist of crystalline domains (means eight-fold coordinated Zr) embedded in the amorphous matrix. Such crystalline domains, we believe that, yield higher coordinated Zr atoms in the experimental samples. It should be noted that the density expansion is about 18% for the metamict zircon while the increase is about 27% for our amorphous configuration. We also believe that the density difference between previous simulations and our simulation is the main factor to witness rather different CN for Zr atoms. In the earlier studies, the constant volume calculations were performed by considering 18% volume expansion while a constant pressure simulation was used in the present work. Yet some factors such as time scale, empirical potentials, size of the simulation cell *etc.* can have some contributions to have different resulting products.

Since our model is significantly different from the metamict zircon (density and CN of Zr atoms), we propose here that it does indeed represent a very low density form of amorphous zircon, which has not been discussed in any earlier investigations.

One might argue that the weakness of our simulation is the responsible for the observation of the low coordinated Zr atoms in the amorphous zircon model. Yet we need to underline here that using the same simulation approaches and parameters (basis, pseudopotentials, etc) we have modeled amorphous zirconia [42] and found that 64% of Zr atoms are seven-fold coordinated, in a contrast to what we find in amorphous zircon. Consequently, we believe that our simulation

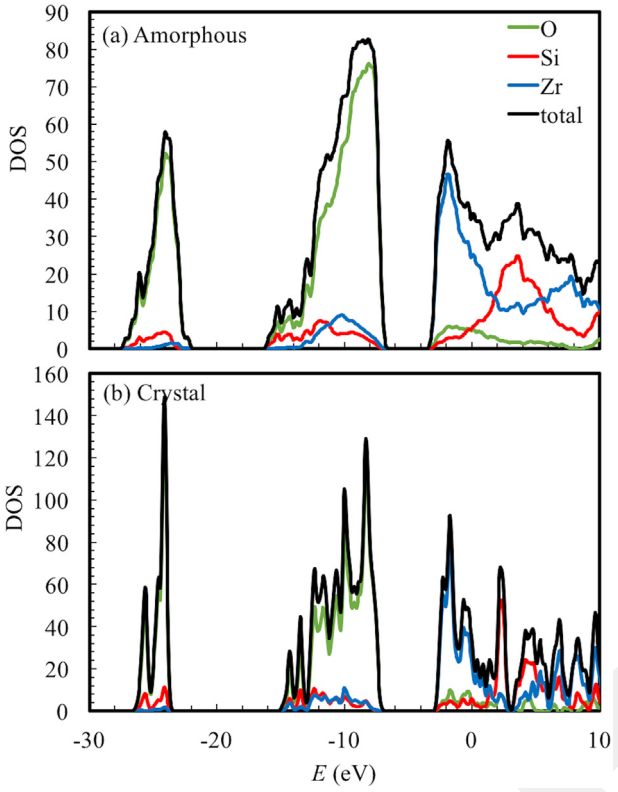

Fig. 10. Total and partial electron density of states of amorphous and crystalline zircon

produces reliable results for amorphous zircon as well.

Finally we would like to underline here that all our findings are based on a 192 atoms model. For models having larger sizes, it might be possible to observe slightly different structured amorphous configurations. Also although we use a quite low quenching rate for *ab initio* simulations, it is rather too fast compared to the cooling rates used in experiments to obtain glassy materials. For different quenching rates, it is also likely to perceive marginally distinctive local structures for amorphous zircon. Therefore, further studies are needed to investigate the impacts of the sizes and quenching rates on the structure of amorphous zircon.

5. Conclusions

Amorphous zircon is generated from the melt using an *ab initio* MD method. We find that amorphization leads to a dramatic volume swelling of 27%. This value is relatively larger than 18% perceived in the metamict zircon. Such a large volume expansion causes a substantial reduction in the mean coordination number of Zr atoms to about 5.66. This value is the lowest one projected to date for amorphous zircon. The volume swelling is, on the other hand, yields no change in the nearest neighbor coordination number of Si atoms *i.e.*, they are still tetrahedrally coordinated. Amorphization produces the polymerization of SiO_4 units and our model shows the highest polymerization with respect to the earlier investigations. On the basis of our observations, we suggest that our amorphous configuration does not illustrate the metamict zircon but a very low density form of amorphous zircon.

Acknowledgements

MD acknowledges financial support from the Abdullah Gül University support foundation, Turkey.

The calculations were run on TÜBİTAK ULAKBİM, High Performance and Grid Computing Center (TRUBA resources).

References

[1] https://geology.com/minerals/zircon.shtml.
[2] B.E. Burakov, E.B. Anderson, M.V. Zamoryanskay, M.A. Yagovkina, E.E. Strykanova, E.V. Nikolaeva, Synthesis and study of 239Pu-doped ceramics based on zircon, (Zr,Pu)SiO_4, and Hafnon, (Hf,Pu)SiO_4, MRS Proc. 663 (2000) France.
[3] R.C. Ewing, Nuclear waste forms for actinides, Proc. Natl. Acad. Sci. U. S. A. 96 (1999) 3432–3439.
[4] X.Q. Cao, R. Vassen, D. Stoever, Ceramic materials for thermal barrier coatings, J. Eur. Ceram. Soc. 24 (2004) 1–10.
[5] B. Yang, B.J. Luff, P.D. Townsend, Cathodoluminescence of natural zircons, J. Phys. Cond. Mat. 4 (1992) 5617–5624.
[6] K. Robinson, G.V. Gibbs, P.H. Ribbe, The structure of zircon: a comparison with garnet, Am. Mineral. 56 (1971) 782–790.
[7] R.J. Finch, J.M. Hanchar, Structure and chemistry.of Zircon and Zircon group minerals, 53 (1) (2003) 1–25.
[8] R.J. Finch, J.M. Hanchar, P.W.O. Hoskin, P.C. Burns, Rare earth elements in synthetic zircon. Part 2. A single-crystal X-ray study of xenotime substitution, Am. Mineral. 86 (2001a) (2001) 681–689.
[9] R.M. Hazen, L.W. Finger, Crystal structure and compressibility of zircon at high pressure, Am. Mineral. 64 (1979) 196–201.
[10] A.F. Reid, A.E. Ringwood, Newly observed high pressure transformations in Mn3O4, CaAl2O4 *and* ZrSiO4, Earth Planet Sci. Lett. 6 (1969) 205–208.
[11] L.G. Liu, High-pressure phase transformations in baddeleyite and zircon, with geophysical implications, Earth Planet Sci. Lett. 44 (1979) 390–396.
[12] K. Kusaba, Y. Syono, M. Kikuchi, K. Fukuoka, Shock behavior of zircon: phase transition to scheelite structure and decomposition, Earth Planet Sci. Lett. 72 (1985) 433–439.
[13] W. Van Westrenen, M.R. Frank, J.M. Hanchar, Y. Fei, R.J. Finch, C.S. Zha, In situ determination of the compressibility of synthetic pure zircon ($ZrSiO_4$) and the onset of the zircon-reidite phase transition, Am. Mineral. 89 (2004) 197–203.
[14] H.P. Scott, Q. Williams, E. Knittle, Ultralow compressibility silicate without highly coordinated silicon, Phys. Rev. Lett. 88 (1) (2001) 1–4.
[15] D. Errandonea, A.B. Garg, Recent progress on the characterization of the high-pressure behaviour of AVO_4 orthovanadates, Prog. Mater. Sci. 97 (2018) 123–169.
[16] R.C. Ewing, A. Meldrum, L. Wang, W.J. Weber, L.R. Corrales, Radiation effects in Zircon, Rev. Mineral. Geochem. 53 (1) (2003) 387–425.
[17] H.D. Holland, D. Gottfried, The effect of nuclear radiation on the structure of zircon, Act. Cry 8 (1955) 291–300.
[18] F. Farges, The structure of metamict zircon- a temperature-dependent EXAFS study, Phys. Chem. Min. 20 (1994) 504–514.
[19] W.J. Weber, R.C. Ewing, L.M. Wang, The radiation-induced crystalline-to-amorphous transition in zircon, J. Mater. Res. 9 (1994) 688–698.
[20] M.A. Russak, C.V. Jahnes, E.P. Katz, Reactive magnetron sputtered zirconium oxide and zirconium silicon oxide thin films, J. Vac. Sci. Technol. A 7 (3) (1989) 1248–1253.
[21] M. Nogami, Glass preparation of the ZrO_2-SiO_2 system by the sol-gel process from metal alkoxides, J. Non-Cryst. Solids 69 (2–3) (1985) 415–423 1985.
[22] R.S. Pavlik, H.J. Holland, E.A. Payzant, Thermal decomposition of zircon refractories, J. Am. Ceram. Soc. 84 (12) (2001) 2930–2936.
[23] J. Du, R. Devanathan, L.R. Corrales, W.J. Weber, A.N. Cormack, Short- and medium-range structure of amorphous zircon from molecular dynamics simulations, Phys. Rev. B 74 (2006) 214204.
[24] R. Devanathan, L.R. Corrales, W.J. Weber, A. Chartier, C. Meis, Molecular dynamics simulation of disordered zircon, Phys. Rev. B 69 (2004) 64115.
[25] E. Balan, I.F. Mauri, C.J. Pickard, I. Farnan, G. Calas, The aperiodic states of zircon: an ab initio molecular dynamic study, Am. Mineral. 88 (2003) 1769–1777.
[26] Siesta manual (4.0) p. 144, http://departments.icmab.es/leem/siesta/Documentation/Manuals
[27] M. Parrinello, A. Rahman, Polymorphic transitions in single crystals: a new molecular dynamics method, J. Appl. Phys. 52 (1981) 7182.
[28] J.P. Perdew, K. Burke, M. Ernzerhof, Generalized gradient approximation made simple, Phys. Rev. Lett. 77 (1996) 3865–3868.
[29] N. Troullierand, J.M. Martins, Efficient pseudo potentials for plane-wave calculations, Phys. Rev. B 43 (1991) 1993–2006.
[30] R. Hundt, J.C. Schön, A. Hannemann, M. Jansen, Determination of symmetries and idealized cell parameters for simulated structures, J. Appl. Crystallogr. 32 (3) (1999) 413–416.
[31] C.B. William, R.F. Wilfrid, Zircon stability and the ZrO_2-SiO_2 phase diagram, Am. Mineral 52 (1967) 880–885.
[32] J.P.H. Williamson, Zircon, Concise Encyclopedia of Advanced Ceramic Materials, 1991, p. 525.
[33] L.R. Sebastien, P. Valery, ISAACS – interactive structure analysis of amorphous and crystalline systems, J. Appl. Crystallogr. 43 (2010) 181–185.
[34] I. Farnan, E. Balan, C.J. Pickard, F. Mauri, The effect of radiation damage on local structure in the crystalline fraction of $ZrSiO_4$: investigating the ^{29}Si NMR response to pressure in zircon and reidite, Am. Mineral. 88 (2003) 1663–1667.
[35] R. Dutta, N. Mandal, Effect of pressure on the elasticity and stability of zircon ($ZrSiO_4$): First-principle investigation, Comp. Mater. Sci. 54 (2012) 157.
[36] J.P. Crocombette, D. Ghaleb, Modeling the structure of zircon ($ZrSiO_4$): empirical potentials, ab initio electronic structure, J. Nucl. Mater. 257 (1998) 282.
[37] Powder Diffraction File PDF-2 Database, PDF 6–266, JCPDS-ICDD, 1998.

[38] B.D. Begg, N.J. Hess, W.J. Weber, S.D. Conradson, M.J. Schweiger, R.C. Ewing, XAS *and* XRD *study of annealed* ^{238}Pu- *and* ^{239}Pu-*substituted zircons* ($Zr_{0.92}Pu_{0.08}SiO_4$), J. Nucl. Mater. 278 (2000) 212–224.
[39] K. Trachenko, M.T. Dove, T. Geisler, I. Todorov, W. Smith, Radiation damage effects and percolation theory, J. Phys. Cond. Mattter 16 (2004) 2623–2627.
[40] V.V. Hoang, Molecular dynamics simulation of amorphous SiO2 nanoparticles, J. Phys. Chem. B 111 (2007) 12649–12656.
[41] J. Robertson, Band offsets of wide-band-gap oxides and implications for future electronic devices, J. Vac. Sci. Technol. B/ Microelectron. Nanometer Struct. 18 (3) (2000) 1785–1791.
[42] M. Durandurdu, Amorphous zirconia: ab initio molecular dynamics simulations, Philos. Mag. 97 (16) (2017) 1334–1345.